Journal of Semiconductors
(2021) 42, 072901
doi: 10.1088/1674-4926/42/7/072901

ARTICLES

Fiber coupled high count-rate single-photon generated from InAs quantum dots

Yao Chen[1, 2, 3], Shulun Li[3, 4, 5], Xiangjun Shang[3, 4, 5], Xiangbin Su[3, 4, 5], Huiming Hao[3, 4, 5], Jiaxin Shen[6], Yu Zhang[3, 4, 5], Haiqiao Ni[3, 4, 5, †], Ying Ding[1, 2, 3, †], and Zhichuan Niu[3, 4, 5, †]

[1]State Key Laboratory of Photon-Technology in Western China Energy, Northwest University, Xi'an 710069, China
[2]Institute of Photonics & Photon-Technology, Northwest University, Xi'an 710069, China
[3]State Key Laboratory for Superlattice and Microstructures, Institute of Semiconductors, Chinese Academy of Sciences, Beijing 100083, China
[4]Center of Materials Science and Optoelectronics Engineering, University of Chinese Academy of Sciences, Beijing 100049, China
[5]Beijing Academy of Quantum Information Sciences, Beijing 100193, China
[6]School of Microelectronics, Xidian University and The State Key Discipline Laboratory of Wide Band Gap Semiconductor Technology, Xi'an 710071, China

Abstract: In this work, we achieve high count-rate single-photon output in single-mode (SM) optical fiber. Epitaxial and dilute InAs/GaAs quantum dots (QDs) are embedded in a GaAs/AlGaAs distributed Bragg reflector (DBR) with a micro-pillar cavity, so as to improve their light emission extraction in the vertical direction, thereby enhancing the optical SM fiber's collection capability (numerical aperture: 0.13). By tuning the temperature precisely to make the quantum dot exciton emission resonant to the micro-pillar cavity mode (Q ~ 1800), we achieve a fiber-output single-photon count rate as high as 4.73×10^6 counts per second, with the second-order auto-correlation $g^2(0)$ remaining at 0.08.

Key words: single-photon source; fiber-output; high count rate

Citation: Y Chen, S L Li, X J Shang, X B Su, H M Hao, J X Shen, Y Zhang, H Q Ni, Y Ding, and Z C Niu, Fiber coupled high count-rate single-photon generated from InAs quantum dots[J]. *J. Semicond.*, 2021, 42(7), 072901. http://doi.org/10.1088/1674-4926/42/7/072901

1. Introduction

The single-photon source has had a significant impact on the development of multiple fields, encompassing quantum information, quantum computing, and quantum communication[1–4]. Epitaxially grown semiconductor QDs and chemical sol QDs are the main methods of achieving single-photon emission from quantum dots[5]. Self-assembled semiconductor QDs have greater advantages[6], such as a higher single-photon emission rate[7], covering visible light to infrared wavelengths[8], and easy embedding in microcavities[9]. However, owing to the fact that many semiconductor materials in the three and five groups have a high refractive index, the total reflection makes collection difficult for many types of quantum dot. As such, various methods have been employed, with the aim of improving collection efficiency. These include micro lenses[10, 11], mesa structures[12, 13], microcavity structures[14], whispering wall structures[15], photonic crystals[16, 17], and nanowire micro-cavities[18]. However, these methods can suffer from processing difficulties, in addition to which, the single photon source cannot be accurately located using these methods.

In this work, we optimize previously-adopted experimental conditions[19], increasing the pairs of DBRs, and employing a phase-matching growth method[20]. In this way, we have greatly improved the intensity of the single photon. In addition, we achieve the direct coupling of a single photon source with a fiber array (this method is easy to operate, and has a high coupling efficiency). In the case of cavity-mode matching (T = 33.6 K), at 918 nm, we collected 4.73×10^6 counts per second (cps) from the fiber end (i.e., 2.5 times the value obtained in previous research[19]), with a time correlation of $g^2(0) = 0.0795$. This confirms that the single-photon source has high intensity and purity. Our method is simple and effective, and still has a lot of room for improvement.

2. Epi-structure and experimental setup

The epitaxial structures were grown on semi-insulating (100) GaAs substrates by means of solid-source molecular beam epitaxy (Veeco Gen930). The Epi-structure of the sample is shown in Fig. 1.

We adopted the subcritical indium deposition technique, together with a gradient indium flux on the static GaAs substrate, to form InAs QDs with top 15 and bottom 25 pairs of GaAs/$Al_{0.9}Ga_{0.1}As$, in order to obtain a high-Q DBR cavity. Although the thickness of the GaAs layer is designed to be 62.57 nm, and the thickness of the $Al_{0.9}Ga_{0.1}As$ layer is designed to be 74.7 nm, we employed phase-matching growth[20] to achieve an accurate thickness measurement. We firstly grew a reference sample, with 6 or 8 pairs of upper DBR, and 10 or 12 pairs of lower DBR. Once growth was completed, the reference sample was immediately taken for testing. On the reference sample, we selected 6–8 positions from

---

Correspondence to: H Q Ni, nihq@semi.ac.cn; Y Ding, yingding@nwu.edu.cn; Z C Niu, zcniu@semi.ac.cn

Received 17 DECEMBER 2020; Revised 27 JANUARY 2021.

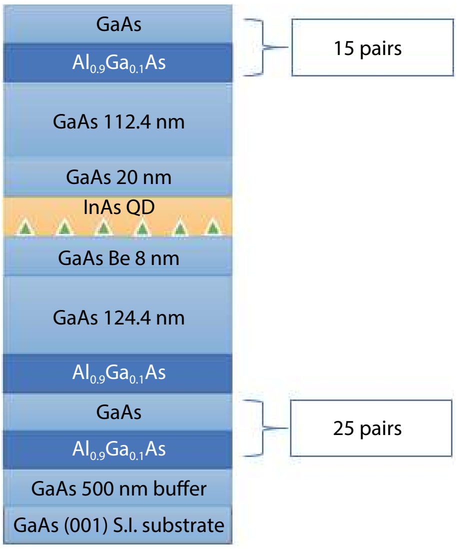

Fig. 1. (Color online) The epi-structure of the sample.

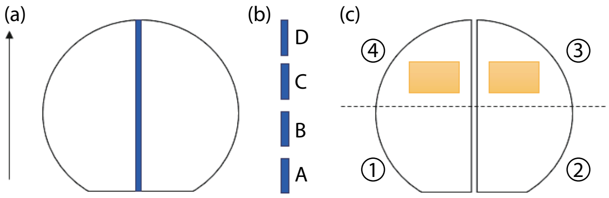

Fig. 2. (Color online) (a) Inscribing a stripe with a narrow ditch on the substrate along the gradient indium flux direction. (b) Dividing the stripe into four small parts (A, B, C, D). (c) Illustrations of selected areas for etching.

the center to the edge, and measured the reflection spectra at these positions. Comparing these reflection spectra with the theoretically designed reflection spectra, we were able to determine whether the actual DBR thickness had become thicker or thinner than the designed value. Having made the corresponding adjustments (increasing or shortening the growth time), we were then able to grow a structure with 15/25 pairs of DBR in the subsequent run. In this way, a more suitable structure can be obtained after only a few runs. The resulting QDs possess a high count rate, and strong vertical light emission.

3. Coupling step

Firstly, we inscribe a stripe with a narrow ditch onto the substrate, along the gradient indium flux direction, and divide it into four small pieces (see Fig. 2(b)), and measure each piece at low temperature (T = 6 K), to locate a QD in a low-density area. If C (A, B, C, D) is a low-density area, the yellow area as shown in Fig. 2(c) is also a low-density area, and the blocks numbered 3 and 4 will be used for the micro-pillar process.

16 single-mode fibers G657, core/cladding diameters: 9 μm/125 μm are embedded in V-grooves with an interval of 127 μm, as shown in Figs. 3(a)–3(c), to form an optical fiber array, designed to be coupled to micropillars. By means of sputtering SiO_2 (as a hard mask), photolithography, and ICP etching, we were able to form micropillars with a diameter of 3 μm, as shown in Fig. 3(d), and an interval of 12 μm.

The substrate with micropillar array was then cut into smaller rectangles. A drop of ultraviolet-curable epoxy (Norland Optical Adhesive 61) was placed on the fiber array facet, then the front side of the substrate was pasted onto the glue, and aligned with the coupling fiber row.

The device is shown in Fig. 4(a): Firstly, one drop of ultraviolet curable epoxy was dripped onto the fiber surface, and a substrate with micropillars was attached to the fiber's surface. Secondly, we used a needle, pressing on the back of the substrate, to reduce the inclination angle between the front of the substrate and the optical fiber. A strong ultraviolet laser (365 nm) pointer then irradiated the coupling for 5–10 s. Once the ultraviolet curable epoxy was cured, the coupling fiber from the pressing device was removed. Thirdly, a few drops of ultraviolet curable epoxy were dripped onto the back of the substrate. The substrate was then placed under an ultraviolet lamp for 4–5 h to consolidate the coupling between the substrate and the optical fiber. Once the ultraviolet curable epoxy was completely cured, we used a metal holder, as shown in Fig. 4(b), to carry and fix the coupling optical fiber. The inside of the metal holder was coated with thermally conductive glue, then the coupling optical fiber was inserted into the thermally conductive glue, and finally fixed with screws.

We used the JANIS CCS-100 device for our preliminary test. This device can measure the PL spectrum of 16 fibers at a time, but its temperature control accuracy is low, and the temperature cannot be changed arbitrarily. At a temperature of about 35 K, we located QDs of superior intensity and quality, as shown in Fig. 5(a). They exhibit good monochromaticity, with no influence from other nearby QDs. In contrast, Fig. 5(b) shows a bad coupling position, where photons from many QDs are coupled to the same fiber.

Finally, the higher-quality coupling groups are tested separately on a more accurate temperature control platform, with the same experimental setup[19]. The setup can now accurately control a range of sample temperatures (4–40 K). This setup can only test one fiber at a time, but can accurately control the temperature, and change the sample temperature during the test. This is extremely important for testing, because many samples are at a certain temperature, and the light intensity can reach the highest value.

4. Results and discussion

We find that a change in temperature has an obvious effect on the matching degree of the cavity mode, as well as single QD excitation (X). The cavity-mode (CM) matching requires precise temperature control. The fitting results for the PL spectra under different temperature conditions are shown in Fig. 6.

Fig. 6(a) shows the fitting for cavity-mode mismatching, at a temperature of 27.4 K. Fig. 6(b) shows the fitting for cavity-mode matching, at a temperature of 33.6 K.

Fig. 7 depicts a three-dimensional graph, based on measuring and fitting a set of variable-temperature PL-spectrum data. The figure clearly shows that when the cavity mode overlaps the single QD excitation (X), the luminosity efficiency reaches its maximum.

As shown in Fig. 8, when the cavity is matched with single QD excitation (X), by changing the excitation power, measuring the intensity of a single photon and cavity mode re-

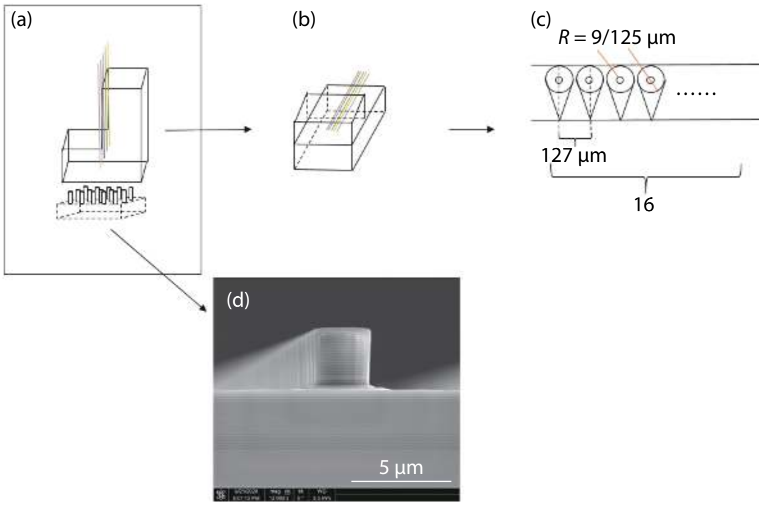

Fig. 3. Schematic diagrams of (a) fiber coupling, (b) fiber array, (c) cross-section of optical fiber array. (d) SEM image of micropillar array.

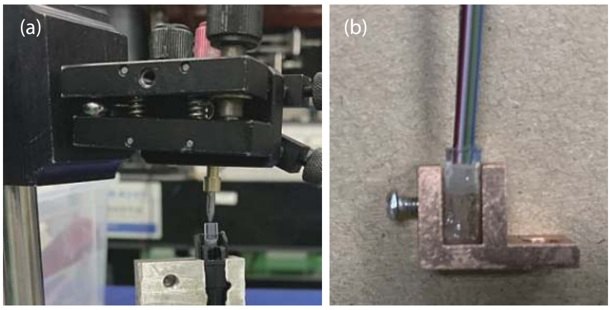

Fig. 4. (Color online) (a) Auxiliary coupling device. (b) The coupled fiber array is fixed onto the metal holder.

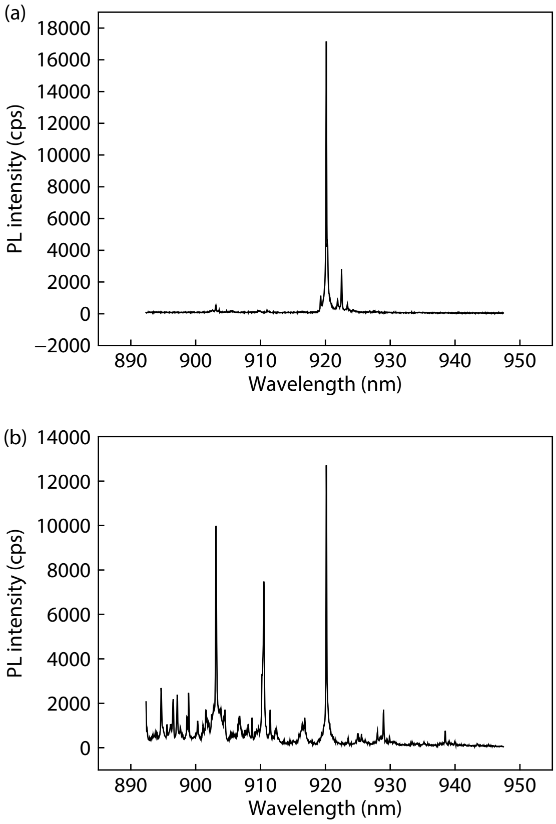

Fig. 5. (a) Single photon coupled by the SM fiber at preliminary testing. (b) Multiple photons, coupled by one fiber.

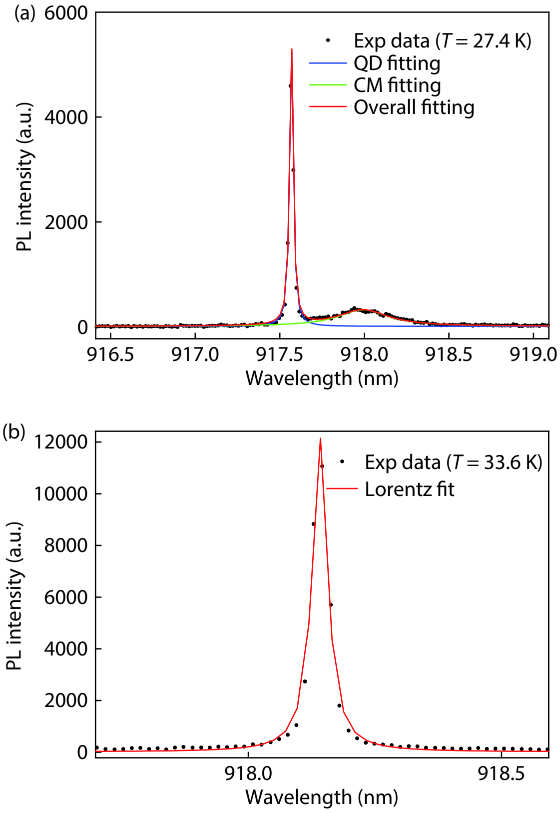

Fig. 6. (Color online) (a) Cavity modes are mismatched at 27.4 K (with p200 attenuation), using the Lorentz function fit for the PL spectrum. (b) Cavity modes matched at 33.6 K (with p200 attenuation), fitting the PL spectrum.

veals the linear relationship ($I \propto P^n$). This demonstrates the emission characteristics of the QD.

In order to prove that the single-photon source has good anti-beam properties, the second-order correlation function is calculated by means of the Hanbury Brown–Twiss (HBT) experiment. We measured cavity-mode resonance and cavity-mode mismatch respectively, as shown in Fig. 9.

In the case of cavity-mode mismatching (T = 32.4 K), the single-channel APD received count rate is 59 000. After deconvolution fitting, $g^2(0)$ = 0.0817. Fig. 9(a) shows the spectrum corresponding to a temperature of 32.4 K, and Fig. 9(c)

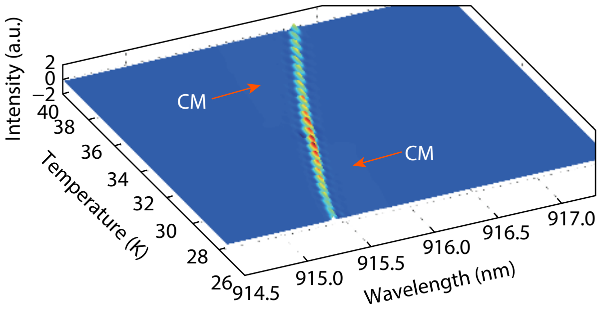

Fig. 7. (Color online) (a) Three-dimensional PL spectrum with variable temperature from 27.4 to 40.4 K.

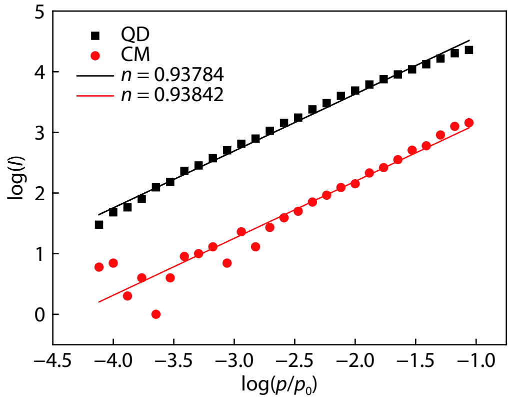

Fig. 8. Intensity of single QD excitation (X) as the excitation power changes, where $I \propto p^{0.9378}$, and the intensity of CM ($I \propto p^{0.9384}$).

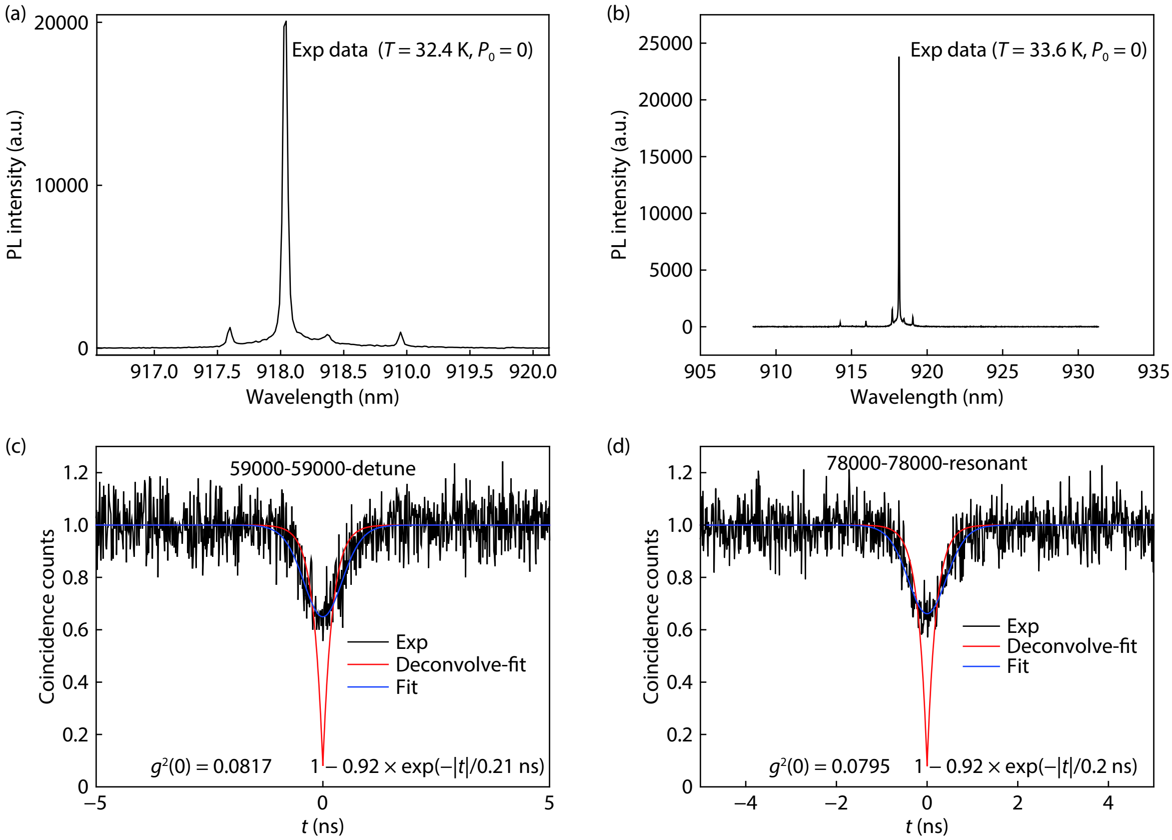

Fig. 9. (a) Spectrum when the sample temperature is 32.4 K (with p_0 attenuation). (b) Spectrum when the sample temperature is 33.6 K (with p_0 attenuation). (c) The second-order correlation function of deconvolved data in the case of fitting cavity-mode mismatching (T = 32.4 K). (d) The second-order correlation function of deconvolved data in the case of fitting cavity-mode matching (T = 33.6 K).

corresponds to the HBT measurement result. In the case of cavity-mode matching (T = 33.6 K), the single-channel APD count rate reaches 78 000, $g^2(0)$ = 0.0795. The results show that our single-photon source has a high single-photon purity. Fig. 9(b) corresponds to the spectrum of the emitted light at a temperature of 33.6 K, and Fig. 9(d) shows the corresponding HBT result.

Lastly, we calculated various optical path losses (including an optical fiber HBT optical path efficiency of 10%, and an APD detection efficiency of 33%) when measuring the HBT, finally estimating that the single photon count-rate transmitted in the coupled fiber could be as much as 4.73 × 10^6 (78 000 × 2 / 0.10 / 0.33 = 4.73 × 10^6 cps).

5. Conclusions

We have achieved the transmission of a high count-rate single-photon source in SM optical fiber by optimizing QD growth conditions and measurements via precise temperature control. The single photon count rate at the fiber end reaches 4.7 × 10^6 cps, and the second-order autocorrelation coefficient, $g^2(0)$, is 0.08 for the resonance of the QD exciton and cavity mode. This coupling method is scalable, and has the potential for significant further improvement.

Acknowledgements

This work is supported by the Key-Area Research and Development Program of Guangdong Province (Grant No.

2018B030329001), the National Key Technologies R&D Program of China (2018YFA0306101), The Scientific Instrument Developing Project of the Chinese Academy of Science (YJKYYQ20170032), the National Natural Science Foundation of China (61505196), and the Program of Beijing Academy of Quantum Information Sciences (Grant No.Y18G01).

References

[1] Kroutvar M, Ducommun Y, Heiss D, et al. Optically programmable electron spin memory using semiconductor quantum dots. Nature, 2004, 432, 81

[2] Cade N I, Gotoh H, Kamada H, et al. Optical characteristics of single InAs/InGaAsP/InP(100) quantum dots emitting at 1.55 μm. Appl Phys Lett, 2006, 89, 181113

[3] He Y M, He Y, Wei Y J, et al. On-demand semiconductor single-photon source with near-unity indistinguishability. Nat Nano, 2013, 8, 213

[4] Faraon A, Fushman I, Englund D, et al. Coherent generation of non-classical light on a chip via photon-induced tunnelling and blockade. Nat Phys, 2008, 4, 859

[5] Sebald K, Michler P, Passow T, et al. Single-photon emission of CdSe quantum dots at temperatures up to 200 K. Appl Phys Lett, 2002, 81, 2920

[6] Shan G C, Yin Z Q, Shek C H, et al. Single photon sources with single semiconductor quantum dots. Front Phys, 2014, 9, 170

[7] Gazzano O, de Vasconcellos S M, Arnold C, et al. Bright solid-state sources of indistinguishable single photons. Nat Commun, 2013, 4, 1425

[8] Buckley S, Rivoire K, Vučković J. Engineered quantum dot single-photon sources. Rep Prog Phys, 2012, 75, 126503

[9] Lodahl P, van Driel A F, Nikolaev I S, et al. Controlling the dynamics of spontaneous emission from quantum dots by photonic crystals. Nature, 2004, 430, 654

[10] Ma Y, Kremer P E, Gerardot B D. Efficient photon extraction from a quantum dot in a broad-band planar cavity antenna. J Appl Phys, 2014, 115, 023106

[11] Fischbach S, Schlehahn A, Thoma A, et al. Single quantum dot with microlens and 3D-printed micro-objective as integrated bright single-photon source. ACS Photonics, 2017, 4, 1327

[12] Miyazawa T, Takemoto K, Sakuma Y, et al. Single-photon generation in the 1.55-μm optical-fiber band from an InAs/InP quantum dot. Jpn J Appl Phys, 2005, 44, L620

[13] Takemoto K, Takatsu M, Hirose S, et al. An optical horn structure for single-photon source using quantum dots at telecommunication wavelength. J Appl Phys, 2007, 101, 081720

[14] Purcell E M. Spontaneous emission probabilities at radio frequencies. Phys Rev, 1946, 69, 681

[15] Rayleigh L. CXII. The problem of the whispering gallery. Lond Edinb Dublin Philos Mag J Sci, 1910, 20, 1001

[16] Kors A, Fuchs K, Yacob M, et al. Telecom wavelength emitting single quantum dots coupled to InP-based photonic crystal microcavities. Appl Phys Lett, 2017, 110, 031101

[17] Chang W H, Chen W Y, Chang H S, et al. Efficient single-photon sources based on low-density quantum dots in photonic-crystal nanocavities. Phys Rev Lett, 2006, 96, 117401

[18] Claudon J, Bleuse J, Malik N S, et al. A highly efficient single-photon source based on a quantum dot in a photonic nanowire. Nat Photon, 2010, 4, 174

[19] Ma B, Chen Z S, Wei S H, et al. Single photon extraction from self-assembled quantum dots via stable fiber array coupling. Appl Phys Lett, 2017, 110, 142104

[20] Li S L, Chen Y, Shang X J, et al. Boost of single-photon emission by perfect coupling of InAs/GaAs quantum dot and micropillar cavity mode. Nanoscale Res Lett, 2020, 15, 145

Yao Chen studies at Institute of Photonics & Photon-Technology, Northwest University of China. He is mainly engaged in research on semiconductors including single-photon source growth and semiconductor process.

Haiqiao Ni received B. E. and M. E. degrees in material science and engineering from Beijing University of Aeronautics and Astronautics in 1992 and 1995. He received Ph. D. degree in electrical engineering from National University of Singapore in 2002. In 2002, he joined Institute of Semiconductors, Chinese Academy of Sciences as a post-doctor and now as a researcher. His research interests include growth and characterization of InGaNAs(Sb) QWs, InAs QDs, metamorphic structures by MBE, devices for optical communications.

Ying Ding received Ph.D. degree in microelectronics and solid state electronics from the Institute of Semiconductors, Chinese Academy of Sciences. From 2005 to 2017, he worked in Hokkaido University, Nanyang Technological University, University of Dundee, and University of Glasgow. Now he is working with Northwest University as an Adjunct Professor. He is also a visiting Research Fellow with the Institute of Semiconductors, Chinese Academy of Sciences.